NUMERICAL INVESTIGATION OF ENTROPY GENERATION IN LAMINAR FORCED CONVECTION FLOW OVER INCLINED BACKWARD AND FORWARD FACING STEPS IN A DUCT UNDER BLEEDING CONDITION

by

Meysam ATASHAFROOZ, Seyyed Abdolreza GANDJALIKHAN NASSAB, and Amir Babak ANSARI

Mechanical Engineering Department, School of Engineering, Shahid Bahonar University, Kerman, Iran

Original scientific paper
DOI: 10.2298/TSCI110531026A

A numerical investigation of entropy generation in laminar forced convection of gas flow over a recess including two inclined backward and forward facing steps in a horizontal duct under bleeding condition is presented. For calculation of entropy generation from the second law of thermodynamics in a forced convection flow, the velocity and temperature distributions are primary needed. For this purpose, the 2-D Cartesian co-ordinate system is used to solve the governing equations which are conservations of mass, momentum, and energy. These equations are solved numerically using the computational fluid dynamic techniques to obtain the temperature and velocity fields, while the blocked region method is employed to simulate the inclined surface. Discretized forms of these equations are obtained by the finite volume method and solved using the SIMPLE algorithm. The numerical results are presented graphically and the effects of bleeding coefficient and recess length as the main parameters on the distributions of entropy generation number and Bejan number are investigated. Also, the effect of Reynolds number and bleeding coefficient on total entropy generation which shows the amount of flow irreversibilities is presented for two recess length. The use of present results in the design process of such thermal system would help the system attain the high performance during exploitation. Comparison of numerical results with the available data published in open literature shows a good consistency.

Key words: *entropy generation, bleeding, laminar forced convection, backward and forward facing steps, recess*

Introduction

One of the primary objectives in the design of any energy system is to conserve the useful energy in a certain process. The irreversibilities associated within the process components destroy the useful energy. It is clear that the irreversibility cannot be avoided completely because of the second law of thermodynamics, but it can be minimized in order to save the avail-

* Corresponding author; e-mail: ganj110@mail.uk.ac.ir

able energy. Entropy generation analysis provides a useful tool to identify the irreversibilities in any thermal system as well as to determine the optimum condition for any process. Heat transfer and viscous dissipation are the only sources of entropy generation in forced convection flow. Separated flows accompanied with heat transfer are frequently encountered in several engineering applications, such as gas turbines, heat exchangers, combustion chambers, and ducts used in industrial applications. These types of flow are intrinsically irreversible because of the viscous dissipation, separation and re-circulation.

The flow over backward-facing step (BFS) has the most features of separated flows. There are many studies in which the BFS flows were analyzed from a fluid mechanics or a heat transfer perspective. Although the geometry of BFS flow is very simple, the heat transfer and fluid flow over this type of step contain most of complexities. Consequently, it has been used in the benchmark investigations. There are many studies about laminar convection flow over BFS in a duct by several investigators [1-4]. Kondoh *et al*. [5] studied laminar heat transfer in a separating and re-attaching flow, by simulating the flow and heat transfer downstream of a backward-facing step, numerically. The effects of channel expansion ratio, Reynolds number and Prandtl number on heat transfer behavior were investigated. Uruba *et al*. [6] investigated control of narrow channel flow behind a backward-facing step by blowing and suction near the step foot, experimentally. The intensity of flow control is characterized by the suction/blowing flow coefficient. Results indicated that both blowing and suction are able to reduce the length of the separation zone down to one third of its value without control. Besides, it was found that the existing 3-D vortex structures near the step are influenced by suction more then by blowing. A review of research on laminar convection flow over backward and forward facing steps was done by Abu-Mulaweh [7]. In that study, a comprehensive review of such flows, that have been reported in several studies in the open literature was presented. The purpose was to give a detail summary of the effect of several parameters such as step height, Reynolds number, Prandtl number, and the buoyancy force on the flow and temperature distributions downstream of the step. Several correlation equations reported in many studies were also summarized.

Although there are many research studies about BFS geometries, the fluid flow with heat transfer over forward facing step (FFS) received less attention in comparison to the convection flow over BFS. In FFS flow, depending on the magnitude of the flow Reynolds number and geometrical factors, one or two separated flow regions may develop adjacent to the step surface. These separated flow regions make this geometry more complicated to study than the BFS flow in which only one separated flow region occurs behind the step. Owing to this fact, very limited number of research works has investigated the laminar convection flow over FFS in contrast to the BFS geometry. Atashafrooz *et al*. [8] studied laminar forced convection of gas flow over a recess including two backward and forward facing steps in a horizontal duct subjected to bleeding condition. The computational fluid dynamic (CFD) techniques were used to solve the governing equations. The effects of bleeding coefficient and recess length on the flow and heat transfer behaviors of the system are investigated.

Investigation of entropy generation in the flow over BFS and FFS has many engineering applications, such as computation of irreversibility and energy loss in separated regions encountered in flow over gas turbine blades where both viscous effect and heat transfer are presented. Bejan [9, 10] showed that entropy generation in convective fluid flow is due to heat transfer and viscous shear stresses. Numerical studies on the entropy generation in convective heat transfer problems were carried out by different researchers. A numerical solution procedure for predicting local entropy generation for a fluid impinging on a heated wall was developed by

Drost and White [11]. Abu-Nada [12-14] analyzed the convection flow over backward facing step in a duct to investigate the amount of entropy generation in this type of flow. In that work, the set of governing equations were solved by the finite volume method and the distributions of entropy generation number, friction coefficient and Nusselt number on the duct walls were calculated. Moreover, the effect of suction and blowing on the entropy generation number and Bejan number were presented. In a recent study, Bahrami and Gandjalikhan Nassab [15] analyzed the convection flow over forward facing step in a duct to investigate the amount of entropy generation in this type of flow. In the other different study, a 3-D original numerical study of entropy generation in the case of liquid metal laminar natural convection in a differentially heated cubic cavity and in the presence of an external magnetic field orthogonal to the isothermal walls was carried out by Kolsi *et al*. [16]. The effect of this field on the various types of irreversibilities was analyzed in that work.

In all mentioned studies, the step was considered to be vertical to the bottom wall. There are many engineering applications in which the forward or backward facing step is inclined. In a recent study, Gandjalikhan Nassab *et al*. [17] studied the turbulent forced convection flow adjacent to inclined forward facing step in a duct. In that study, the Navier-Stokes and energy equations were solved in the computational domain by CFD method using conformal mapping technique. By this method, the effect of step inclination angle on flow and temperature distributions was determined. Ansari and Gandjalikhan Nassab [18] studied the laminar forced convection flow of a radiating gas adjacent to inclined forward facing step in a duct. In that study the blocked region method was used to simulate the inclined step. The effect of radiative parameters on thermal behavior of fluid flow was also studied. Ansari and Gandjalikhan Nassab [19] analyzed laminar forced convection flow of a radiating gas over an inclined backward facing step in a horizontal duct subjected to bleeding condition. The fluid was treated as a gray, absorbing, emitting and scattering medium. The 2-D Cartesian co-ordinate system was used to simulate flow over inclined surface by considering the blocked region in regular grid. The effect of radiative propertied on heat transfer behavior of fluid flow was investigated.

Although there are some studies about entropy generation in many process components such as BFS and FFS flow, a careful inspection of the literature shows that the entropy generation in convection flow over inclined backward and forward facing steps, which provides a recess in a horizontal duct with considering bleeding condition, is still not studied. Therefore, the present research work deals with the investigation of entropy generation in the forced convection flow adjacent to inclined backward and forward facing steps in a 2-D horizontal duct with bottom permeable wall. Toward this end, the set of governing equations are conservations of mass, momentum, and energy are solved by the CFD technique in the Cartesian co-ordinate system, using the blocked region technique in simulating the inclined surfaces.

Theory

2-D laminar forced convection of gas flow in a 2-D horizontal heated rectangular duct over a recess is numerically simulated. Schematic of the computational domain is shown in fig. 1. The upstream and downstream heights of the duct are h_1 and h_2, respectively. The height of the duct inside the recess region is H such that this geometry provides the step height of s, with expansion ratio ($ER = H/h_1$) and contraction ratio ($CR = h_2/H$) of 2 and 0.5, respectively. The upstream length of the duct is considered to be L_1=10H and the rest of the channel length is equal to L_2 = 40 H. This is made to ensure that the flow at the inlet and outlet section is not affected significantly by the sudden changes in the geometry and flow at the exit section becomes fully de-

veloped. The recess bottom wall is considered permeable (see fig. 1). The length of permeable wall with bleeding depicted by D is considered to be $5H$ and $20H$ in the test cases. The arrows that are shown at the permeable wall represent the direction of mass bleed through the wall, such that inward and outward directions represent blowing and suction, respectively. Also, the step inclination angle indicated by ϕ is considered to be 45° for both steps in all subsequent calculations.

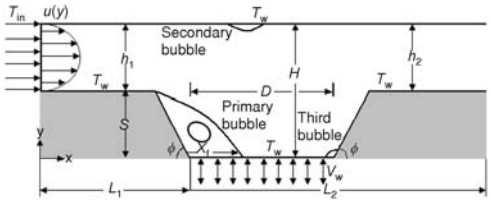

Figure 1. Schematic of computational domain

Basic equations

For incompressible, steady and 2-D laminar flow, the governing equations are the conservations of mass, momentum and energy that can be written as:

$$\frac{\partial u}{\partial x}+\frac{\partial v}{\partial y}=0 \tag{1}$$

$$u\frac{\partial u}{\partial x}+v\frac{\partial u}{\partial y}=-\frac{1}{\rho}\frac{\partial p}{\partial x}+\frac{\mu}{\rho}\left(\frac{\partial^2 u}{\partial x^2}+\frac{\partial^2 u}{\partial y^2}\right) \tag{2}$$

$$u\frac{\partial v}{\partial x}+v\frac{\partial v}{\partial y}=-\frac{1}{\rho}\frac{\partial p}{\partial y}+\frac{\mu}{\rho}\left(\frac{\partial^2 v}{\partial x^2}+\frac{\partial^2 v}{\partial y^2}\right) \tag{3}$$

$$u\frac{\partial T}{\partial x}+v\frac{\partial T}{\partial y}=\alpha\left(\frac{\partial^2 T}{\partial x^2}+\frac{\partial^2 T}{\partial y^2}\right) \tag{4}$$

In eqs. (1)-(4), u and v are the velocity components in x- and y-directions, respectively, ρ – the density, p – the pressure, T – the temperature, μ – the dynamic viscosity, and α – the thermal diffusivity.

Boundary conditions

The boundary conditions are treated as no slip conditions at the solid walls (zero velocity) and constant temperature of T_w at the bottom and top walls including the step surfaces. At the inlet duct section, the flow is fully developed with uniform temperature T_{in}, which is assumed to be lower than T_w. At the porous bottom wall in the recess region, the fluid is allowed to bleed with uniform velocity v_w. Besides, at the outlet section, zero axial gradients for velocity components and gas temperature are employed.

Non-dimensional forms the governing equations

In numerical solution of the set of governing equations including the continuity, momentum, and energy, the following dimensionless parameters are used to obtain the non-dimensional forms of these equations:

$$(X,Y)=\left(\frac{x}{D_h},\frac{y}{D_h}\right),\quad (U,V)=\left(\frac{u}{U_0},\frac{v}{U_0}\right),\quad P=\frac{p}{\rho U_0^2},\quad v_w^*=\frac{v_w}{U_0},\quad \sigma=\frac{v_w}{U_0}$$
$$\Theta=\frac{T-T_{in}}{T_w-T_{in}},\quad \mathrm{Pr}=\frac{v}{\alpha},\quad \mathrm{Re}=\frac{\rho U_0 D_h}{\mu},\quad \mathrm{Pe}=\mathrm{RePr} \tag{5}$$

where D_h is the hydraulic diameter which is equal to $2h_1$. The non-dimensional forms of the governing equations are as follows:

$$\frac{\partial U}{\partial X}+\frac{\partial V}{\partial Y}=0 \tag{6}$$

$$\frac{\partial}{\partial X}\left(U^2-\frac{1}{\mathrm{Re}}\frac{\partial U}{\partial X}\right)+\frac{\partial}{\partial Y}\left(UV-\frac{1}{\mathrm{Re}}\frac{\partial U}{\partial Y}\right)=-\frac{\partial P}{\partial X} \tag{7}$$

$$\frac{\partial}{\partial X}\left(UV-\frac{1}{\mathrm{Re}}\frac{\partial V}{\partial X}\right)+\frac{\partial}{\partial Y}\left(V^2-\frac{1}{\mathrm{Re}}\frac{\partial V}{\partial Y}\right)=-\frac{\partial P}{\partial Y} \tag{8}$$

$$\frac{\partial}{\partial X}\left(U\Theta-\frac{1}{\mathrm{Pe}}\frac{\partial \Theta}{\partial X}\right)+\frac{\partial}{\partial Y}\left(V\Theta-\frac{1}{\mathrm{Pe}}\frac{\partial \Theta}{\partial Y}\right)=0 \tag{9}$$

Positive values of bleed coefficient correspond to blowing and negative values correspond to suction and zero value of bleed coefficient corresponds to impermeable wall. Therefore, the non-dimensional velocity at the porous segment is equal to the bleed coefficient, which is expressed as:

$$\sigma = v_w^* \tag{10}$$

Entropy generation

In the present study, physical quantities of interest in flow field and heat transfer study are the entropy generation and Bejan number.

The following dimensionless quantities are defined:

$$Ns=\frac{s''_{\mathrm{gen}}D_h^2}{\kappa\tau^2},\quad \tau=\frac{T_w-T_{\mathrm{in}}}{T_{\mathrm{in}}},\quad \mathrm{Br}=\frac{\mu U_0^2}{\kappa(T_w-T_{\mathrm{in}})},\quad \Psi=\frac{\mathrm{Br}}{\tau} \tag{11}$$

wher Ns is the entropy generation number, s''_{gen} – the volume rate of entropy generation, Br – the Brinkman number, and τ – the non-dimensional temperature parameter. Using parameters, the entropy generation in dimensionless form can be expressed as [14]:

$$Ns=\left[\left(\frac{\partial\Theta}{\partial X}\right)^2+\left(\frac{\partial\Theta}{\partial Y}\right)^2\right]+\Psi\left\{2\left[\left(\frac{\partial U}{\partial X}\right)^2+\left(\frac{\partial V}{\partial Y}\right)^2\right]+\left[\left(\frac{\partial U}{\partial Y}\right)+\left(\frac{\partial V}{\partial X}\right)\right]^2\right\} \tag{12}$$

This equation is used to solve the entropy generation number at each grid point in the flow domain. Equation (12) contains two parts. The first term on the right hand side represents entropy generation due to the heat transfer:

$$Ns_{\mathrm{cond}}=\left[\left(\frac{\partial\Theta}{\partial X}\right)^2+\left(\frac{\partial\Theta}{\partial Y}\right)^2\right] \tag{12a}$$

whereas the second term represents the entropy generation due to the fluid viscous effect :

$$Ns_{\mathrm{visc}}=\Psi\left\{2\left[\left(\frac{\partial U}{\partial X}\right)^2+\left(\frac{\partial V}{\partial Y}\right)^2\right]+\left[\left(\frac{\partial U}{\partial X}\right)+\left(\frac{\partial V}{\partial X}\right)\right]^2\right\} \tag{12b}$$

The Bejan number which is also computed in the present analysis, shows the relative portion of heat transfer entropy generation to total entropy generation such that Be = 1 means that no viscous entropy generation exist in the flow domain. The Bejan number is defined as:

$$\mathrm{Be} = \frac{Ns_{\mathrm{cond}}}{Ns_{\mathrm{cond}} + Ns_{\mathrm{vics}}} \tag{13}$$

Also, the total entropy generation that can show the amount of irreversibilities due to both viscous friction and heat transfer can be expressed as:

$$Ns = \int_{\forall} Ns(X, Y)\mathrm{d}\forall \tag{14}$$

where $\forall$ is the volume of flow domain.

Numerical procedure

Finite difference forms of the partial differential eqs. (6) to (9) were obtained by integrating over an elemental cell volume with staggered control volumes for the x- and y-velocity components. Other variables of interest were computed at the grid nodes. The discretized forms of the governing equations were numerically solved by the SIMPLE algorithm of Patankar and Spalding [20]. Numerical calculations were performed by writing a computer program in FORTRAN. Based on the result of grid tests for obtaining the grid-independent solutions, six different meshes were used in the grid independence study. The corresponding value of maximum entropy generation on the bottom wall and also the location of re-attachment point are calculated and tabulated in tab. 1. As it is seen, a grid size of 800×40 can be chosen for obtaining the grid independent solution, such that the subsequent numerical calculations are made based on this grid size. It should be mentioned that near the top, bottom, and step walls clustering is employed in the x- and y-directions for obtaining more accuracy in the numerical calculations. Also, it should be noted that the grid generation is employed for the whole domain restricted by $0 \le X \le 50H$ and $0 \le Y \le H$ (region between two parallel plates) in which two steps are simulated by considering two blocked regions, see fig. 2. The numbers of control volumes inside the active and blocked regions for two recess lengths are showed in tab. 2. Numerical solutions are obtained iteratively using the line-by-line method. About the convergency, it should be mentioned that the iterative process continues until achieving convergence of all dependent variables (velocity, pressure and temperature). The convergence of solution is evaluated using a criterion taken as the values of absolute residuals in the momentum and energy equations less than 10^{-4}, and the normalized errors in the velocity and temperature fields for each node by the following criteria:

Table 1. Grid independence study, Re = 400, ϕ = 45°, $D = 20H$, σ = 0.0

Grid size	Maximum entropy generation	
150 × 10	–	13.011
350 × 20	8.201	13.363
550 × 25	8.630	13.606
700 × 35	8.942	13.802
800 × 40	9.162	13.960
850 × 45	9.168	13.962

$$\mathrm{Error}\Phi = \max\left|\frac{\Phi^{n}(i,j) - \Phi^{n-1}(i,j)}{\Phi^{n}(i,j)}\right| \le 10^{-5}$$

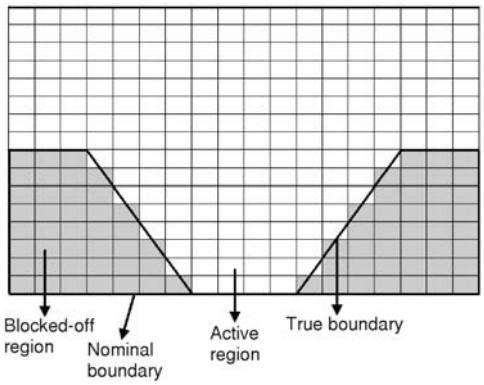

Figure 2. Blocked region in a regular grid

Table 2. The numbers of total, active, and blocked control volumes

D/D_h	20	5
Total control volumes	32000	32000
Active control volumes	24500	20000
Blocked control volumes	7500	12000

where Φ denotes to the velocity components and temperature and n is the iteration level.

By this numerical strategy, the velocity and temperature distributions in the fluid flow can be obtained. After calculation of velocity and temperature fields, eqs. (12) and (13) are used to solve the entropy generation number and Bejan number at each grid point in the flow domain. Then, the total entropy generation through the flow domain is calculated by eq. (14).

Blocked region method

In many cases, a computer program written for a regular grid can be improved to handle an irregularly shaped computational domain using the blocked region method [21-23]. In this method, the whole 2-D region is divided into two parts: active and inactive or blocked regions. The region where solutions are done is known as the active region and the remaining portion is known as the inactive or the blocked region. Therefore, by rendering inactive some of the control volumes of the regular grid, the remaining active control volumes form the desired irregular domain with complex boundary. By this technique, the surface of inclined step in the present analysis is approximated by a series of rectangular steps, fig. 2. It is obvious that using fine grids in the interface region between active and inactive zones causes to have an approximated boundary which is more similar to the true boundary.

According to the blocked region technique, known values of the dependent variables must be established in all inactive control volumes. If the inactive region represents a stationary solid boundary as in the case, the velocity components in that region must be equal to zero, and if the region is regarded as isothermal boundary, the known temperature must be established in the inactive control volumes.

Validation of computational results

As there is not any theoretical result about entropy generation in convection flow over inclined backward and forward facing steps with bleeding condition, the present numerical implementation was validated by reproducing the results of Abu-Nada [14] in which a forced convection flow of gas over a BFS was studied.

In this test case, the bottom wall was permeable with bleeding condition including both suction and blowing. Variation of entropy generation along the bottom wall is compared with that obtained by Abu-Nada [14] at $ER = 2$ and $\mathrm{Re} = 400$ under the presence of blowing. The results are presented graphically in fig. 3. In this test case, the temperature of the top wall was lower than the temperature of the bottom wall and the gas temperature profile at the inlet section was assumed to be fully developed.

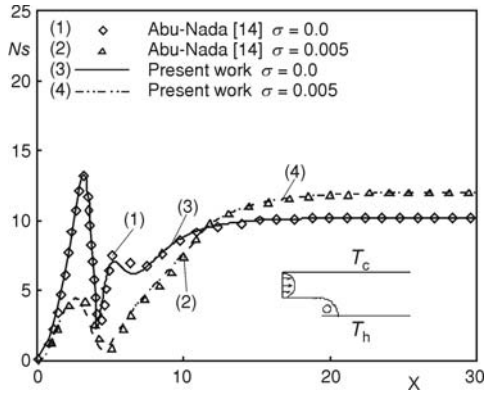

Figure 3. Distribution of entropy generation on the bottom wall

Figure 3 shows that the minimum value of entropy generation occurs at the step corner on the bottom wall, where the fluid has no motion.

Also, this figure shows that the maximum value of *Ns* occurs inside the re-circulation zone and then it drops sharply to a very low value at the re-attachment point. Then *Ns* increases and approaches to a fixed value far from the step. Also, this figure shows that blowing decreases the value of *Ns* inside the re-circulation zone, which is related to the decreased temperature and velocity gradients on the bottom wall. However, fig. 3 shows a good consistency between the present numerical results with those reported by Abu-Nada [14].

Results and discussions

In the present research, numerical results of air flow simulations in a duct with expansion and contraction ratios of $ER = 2$ and $CR = 0.5$, respectively, are considered. In different test cases, two lengths for the recess region are considered with various bleeding rates at Reynolds number equal to 400, while the Prandtl number is kept constant at 0.71 to guarantee the constant fluid physical properties for moderate and small values of temperature difference.

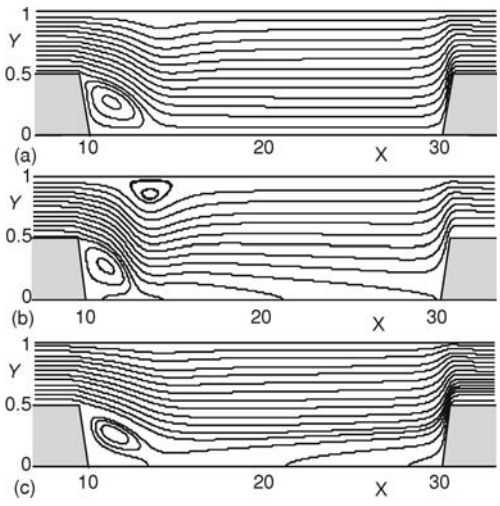

Figure 4. Distribution of stream lines contours, Re = 400; *(a) σ = 0.0, (b) σ = –0.005, (c) σ = 0.005*

For better explanation of results, first the streamlines are plotted in fig. 4 while the recess length is equal to $D = 20H$. The effect of sudden expansion and contraction along the duct is clearly seen from the curvatures of streamlines. Figure 4(a) shows that for Re = 400, the primary re-circulation region occurs downstream of the backward step adjacent the bottom wall. Figures 4(b) and 4(c) show the effect of suction and blowing on the stream lines contours, respectively. It can be seen from these figures that in the case of suction, the re-attachment length decreases whereas the secondary re-circulation zone appears along the top wall. But in the case of blowing, the re-attachment length grows while the secondary bubble disappears.

The variations of entropy generation along the duct walls at Re = 400, $D = 20H$ and in different bleeding coefficient are illustrated in fig. 5. Figure 5(a) shows that the minimum value of entropy generation occurs at the steps corner on the bottom wall, where the fluid is at rest. Also, this figure shows that downstream the step location, the value of *Ns* increases sharply in the primary re-circulation region because of the flow vortices, such that the maximum entropy generation occurs in this re-circulated region. Then, it drops sharply to a very low value at the re-attachment point. Because of zero velocity gradient in

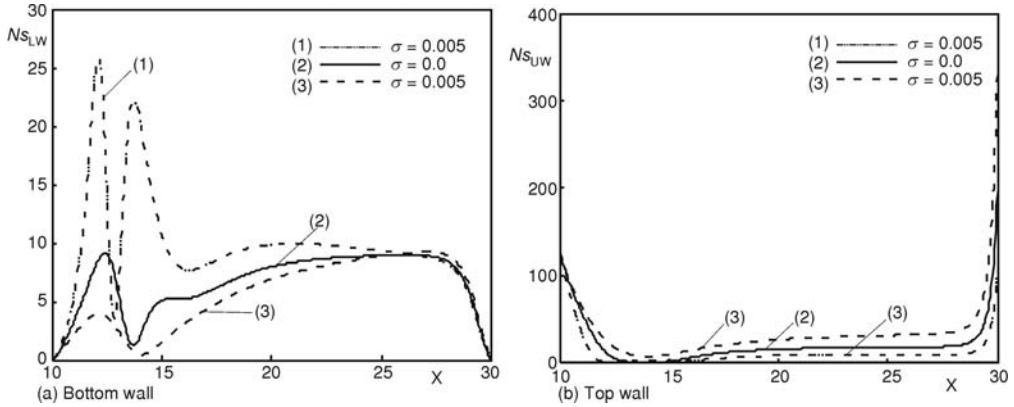

Figure 5. Distribution of entropy generation, Re = 400, $\Psi = 1$, $D = 20H$

the re-attachment point, there are no shear stresses and the viscous contribution in entropy generation is omitted and the value of *Ns* is totally due to conduction heat transfer.

After re-attachment point, entropy generation increases and approaches to a constant value as the distance continues to increase in the stream-wise direction. Finally, the entropy generation decreases along the flow direction such that the value of entropy generation vanishes at the forward step corner where the fluid is at rest. Moreover, fig. 5(a) shows the effect of bleeding coefficient on the distribution of entropy generation along the bottom wall. This figure shows that suction increases the maximum entropy generation while blowing has opposite effect. This is related to the increased temperature and velocity gradients for the case of suction compared to that of blowing. In addition, for the case of suction, the *Ns* reaches a peak after re-attachment point which is due to the appearance of secondary re-circulation on the top wall which narrows down the flow passage and leads to increase in the amount of velocity gradient on the bottom wall. Figure 5(b) represents the distribution of entropy generation on the top wall for various values of the bleeding coefficient. It is obvious that on the top wall the entropy generation starts with high values due to the development of the viscous boundary layer and then *Ns* decreases to a low value. After this local minimum point, *Ns* increases and approaches to a constant value as the distance increases in the stream-wise direction. Finally, the entropy generation increases steeply near the forward step. Also, this figure shows that for the case of blowing, *Ns* on the top wall increases whereas suction has opposite effect.

Figure 6 shows the variation of Bejan number along the duct walls for different values of bleeding coefficient. As it is seen from fig. 6(a), the Bejan number starts from an undefined value at the step corner. In primary re-circulation region, the Bejan number decreases such that the value of Be attains to a low value inside this region. Then, Be increases to its maximum values that occurs at the re-attachment point. As it was mentioned before, the velocity gradient at this point is zero, therefore the viscous contribution in entropy generation is omitted and the value of *N*s is totally due to conduction heat transfer that leads to Be = 1. Under these circumstances Be decreases and reaches a constant value which is due to the fully developed condition and finally increases near the forward step. It is important to note that, for the case of suction Be reaches a small peak after re-attachment point which is due to the existence of the secondary re-circulation region on the top wall. Figure 6(b) shows that Bejan number on the top wall starts at low values due to the development of the boundary layer.

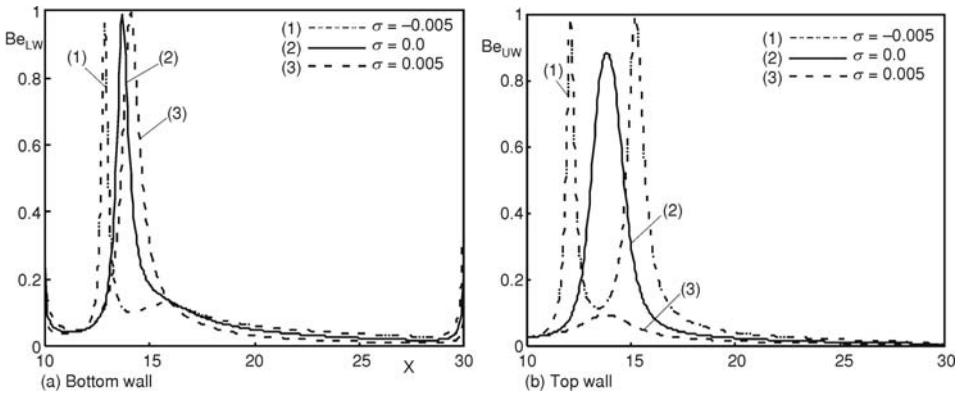

Figure 6. Distribution of Bejan number, Re = 400, $\Psi = 1$, $D = 20H$

Then Bejan number increases and reaches a maximum value inside the secondary re-circulation region and then drops to very low values until Be reaches a small constant value due to the fully developed condition. Also, this figure shows that for the case of suction, the Bejan number on top wall has two peaks which occur at the beginning and end of this bubble such that between these two peaks Be has a low value.

To study the effect of recess length on entropy generation, another test case with the same Reynolds number (Re = 400) is also analyzed for a short recess length with $D = 5H$. To have better view of the flow pattern, the streamlines contours for $D = 5H$ and for three different bleeding coefficients are plotted in fig. 7. Comparing the streamlines in fig. 7 with those plotted in fig. 4, it is observed that the flow field has different patterns in cases of long and short recess lengths. It can be concluded that the recess length has a great effect on the flow pattern. It can be seen from fig. 7 that in the case of no bleeding, because of short recess length, a very small re-circulation region appears near forward step which is called third re-circulation region. But for the cases of suction and blowing, this region disappears, such that for the case of suction, secondary re-circulation bubble also appears on the top wall.

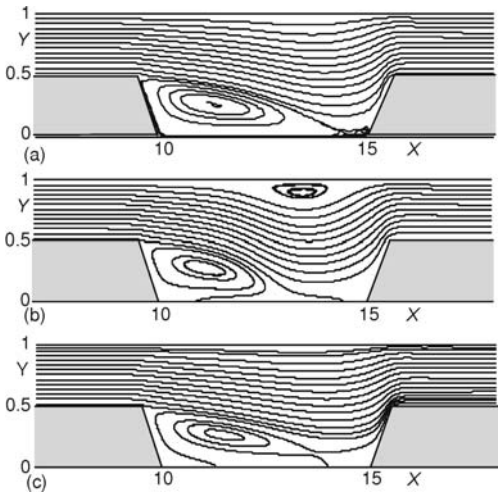

Figure 7. Distribution of stream lines contours, Re = 400, *(a)* $\sigma = 0.0$, *(b)* $\sigma = -0.005$, *(c)* $\sigma = 0.005$

Variation of entropy generation number along the recess bottom wall for the short recess length, $D = 5H$ is plotted in fig. 8. Comparison of this figure with *Ns* distribution shown in fig. 5 illustrates that *Ns* distribution has different trends in short and long recess lengths. Figure 8 indicates that entropy generation increases after the backward step corner in the primary re-circulation region and reaches to its maximum value and then decreases to its minimum value at the forward step corner, where the flow is at rest. Also, this figure shows that for the case of suction,

the maximum entropy generation increases but blowing decreases the maximum entropy generation.

To study the effect of bleeding rate on *Ns* and Be distributions, the variation of entropy generation along the duct wall is plotted in fig. 9 at different suction coefficients. Figure 9(a) shows that by increasing the rate of suction, the maximum entropy generation in primary re-circulation increases and by decreasing suction coefficient, the location of maximum entropy generation moves toward the downstream. Besides it is seen that by increasing in suction coefficient, the value of *Ns* occurs after re-attachment point increases which is due to this fact that by increasing in suction coefficient, the secondary re-circulation bubble developed on the top wall which can be seen obviously in fig.10.

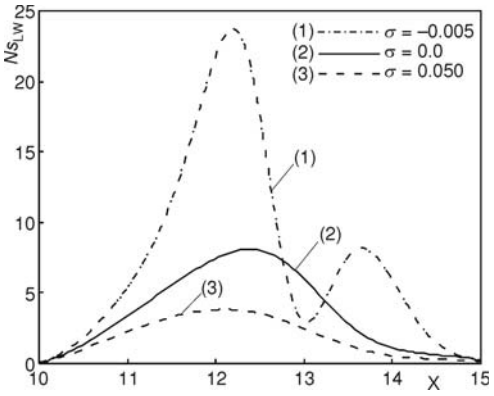

Figure 8. Distribution of entropy generation along the recess bottom wall, Re = 400, Ψ = 1, $D = 5H$

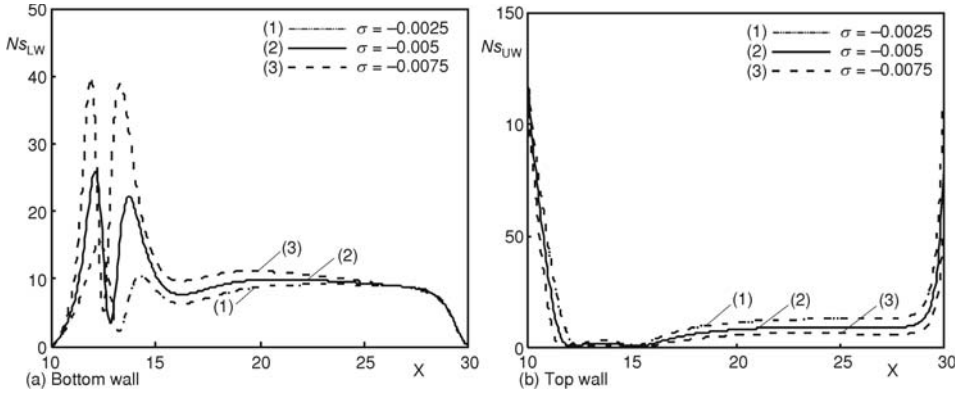

Figure 9. Distribution of entropy generation, Re = 400, Ψ = 1, $D = 20H$

Figure 9(b) shows that by decreasing in suction coefficient, the entropy generation on top wall increases such that near forward step this increasing is great.

Figure 11 shows the effect of suction coefficient on distribution of Bejan number along the duct walls. Figure 11(a) shows that by increasing in suction coefficient, the location of maximum Bejan number on the bottom wall that occurs at the re-attachment point, moves toward the upstream side

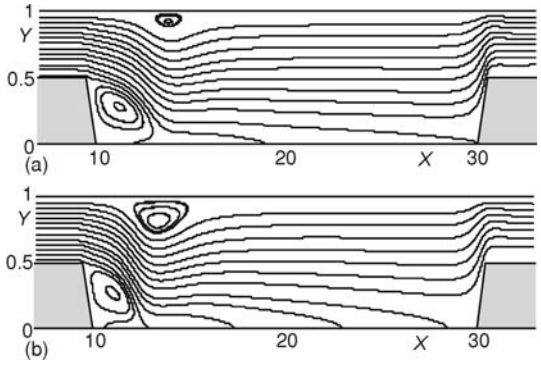

Figure 10. Distribution of stream lines contours, Re = 400, Ψ = 1, $D = 20H$; *(a)* $\sigma = -0.0025$, *(b)* $\sigma = -0.075$

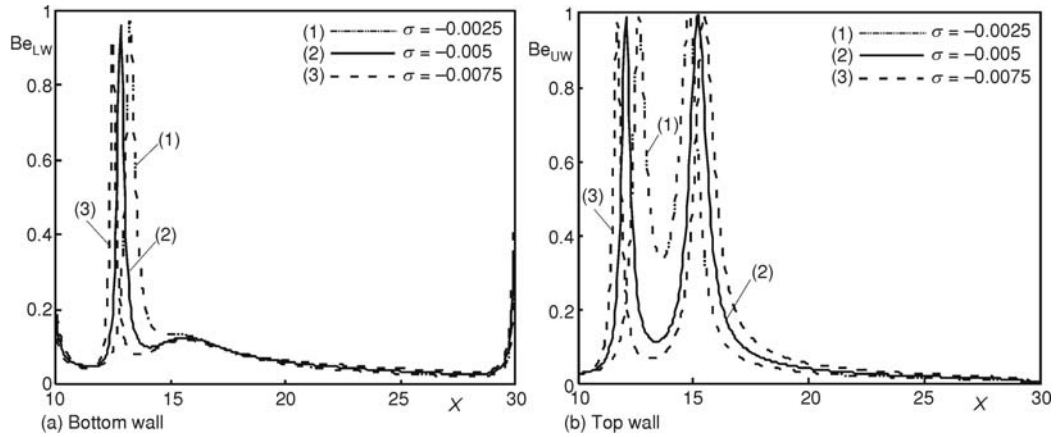

Figure 11. Distribution of Bejan number, Re = 400, $\Psi = 1, \Delta = 20H$

which is due to shortening the length of re-attachment point. Also, fig. 11(b) shows that the maximum Bejan number on the top wall occurs at the beginning and end of the secondary re-circulation bubble, but the distance between these two peaks increases as the suction coefficient increases. Also, the minimum value of Be between these two peaks increases by decreasing in suction coefficient.

As it was mentioned before, the amount of irreversibility in a fluid flow can be shown by computing the total entropy generation in the flow domain. Therefore, to evaluate the value of total entropy generation inside the flow domain under study in the present work restricted by $L_1 \le X \le (L_1 + D)$ and $0 \le Y \le H$ the variation of total entropy generation against the bleeding coefficient for four different values of the Reynolds number and two recess length are presented in fig. 12. This figure illustrates that the value of total entropy generation that shows the amount of flow irreversibility increases with increasing Reynolds number. Also, it is seen that suction and blowing have opposite effects on the total entropy generation number, such that suction decreases and blowing increases the value of total entropy generation in convective flow. Finally,

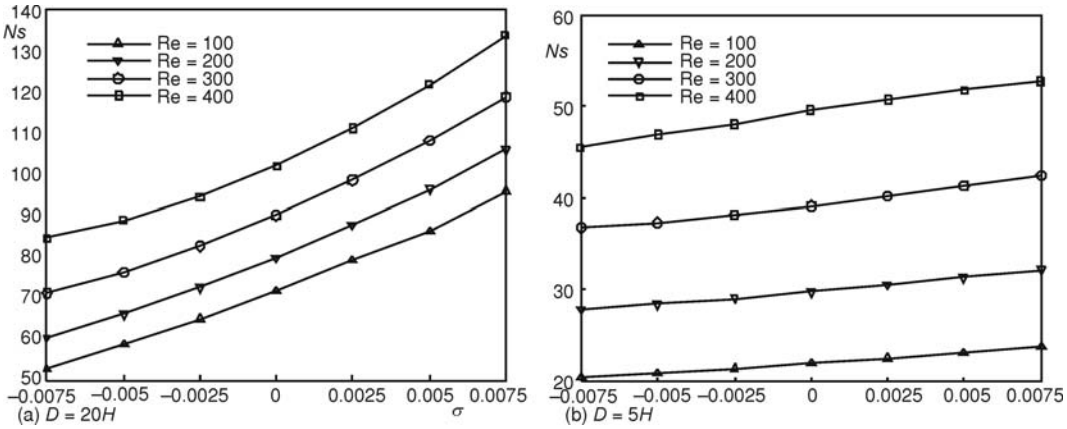

Figure 12. Distribution of total entropy generation with σ, $\Psi = 1$

fig. 12 illustrates that the recess length has a great effect on flow irreversibilities, such that the value of total entropy generation increases sharply with increasing in recess length.

Conclusions

Present study deals with the analysis of entropy generation in forced convection laminar flow over two consequent inclined backward and forward facing steps with constant inclination angle in a 2-D horizontal duct under the presence of bleeding process. The set of governing equations consisting of the conservations of mass, momentum, and energy is solved numerically by the CFD techniques in the Cartesian co-ordinate system using the blocked region method. The effects of bleeding coefficient, Reynolds number, and recess length on entropy generation distribution and Bejan number were investigated. Also, total entropy generation in the flow domain for various bleeding coefficient and different Reynolds numbers in two recess lengths was calculated. It was revealed that the recess length, Reynolds number and bleeding rate have great effect on the entropy generation and flow irreversibility in convection flow in this type of flow geometry. It should be mentioned that by increasing Reynolds numbers, recess length and blowing coefficient, the amount of irreversibility in a fluid flow increases whereas by increasing suction coefficient, the value of this parameter decreases.

Nomenclature

Be – Bejan number
Br – Brinkman number
CR – contraction ratio
D_h – hydraulic diameter, [m]
ER – expansion ratio
Ns – entropy generation number
Pe – Peclet number
Pr – Prandtl number
Re – Reynolds number
s''_{gen} – volume rate of entropy generation
T – temperature, [K]
U_0 – average velocity of the incoming flow at the inlet section, [ms^{-1}]
x, y – horizontal and vertical distance, respectively, [m]
X, Y – dimensionless horizontal and vertical co-ordinate, respectively
x_r – re-attachment length, [m]

Greek symbols

α – thermal diffusivity, [m^2s^{-1}]
Θ – dimensionless temperature
κ – thermal conductivity
μ – dynamic viscosity
ν – kinematic viscosity
ρ – density
τ – dimensionless temperature parameter
ϕ – step inclination angle
Ψ – viscous dissipation number

Subscripts

in – inlet section
w – wall
cond – conduction
visc – viscous
LW – bottom wall
UW – top wall

References

[1] Armaly, B. F., *et al*., Experimental and Theoretical Investigation of Backward-Facing Step Flow, *Journal of Fluid Mechanics, 127* (1983), February, pp. 473-496
[2] Vradis, G., Van Nostrand, L., Laminar Coupled Flow Downstream an Asymmetric Sudden Expansion, *Journal of Thermophysics Heat Transfer, 6* (1992), 2, pp. 288-295
[3] Tylli, N., *et al* ., Side Wall Effects in flow over Backward-Facing Step: Experiments and Numerical Solutions, *Physics Fluids, 14* (2002), 11, pp. 3835-3845
[4] Brakely, D., *et al.,* Three-Dimensional Instability in Flow over a Backward – Facing Step, *Journal of Fluid Mechanics, 473* (2002), December, pp. 167-190
[5] Kondoh, T., *et al.,* Computational Study of Laminar Heat Transfer Downstream of a Backward-Facing Step, *International Journal of Heat and Mass Transfer, 36* (1993), 3, pp. 577-591

[6] Uruba, V., *et al*., Control of a Channel-Flow behind a Backward-Facing Step by Suction/Blowing, *International Journal of Heat and Fluid Flow, 28* (2007), 4, pp. 665-672
[7] Abu-Mulaweh, H. I., A Review of Research on Laminar Mixed Convection Flow over Backward- and Forward-Facing Steps, *International Journal of Thermal Sciences, 42* (2003), 9, pp. 897-909
[8] Atashafrooz, M., *et al*., Numerical Analysis of Laminar Forced Convection Flow over Backward and Forward Facing Steps in a Duct under Bleeding Condition, *International Review of Mechanical Engineering, 5* (2011), 3, pp. 513-518
[9] Bejan, A., A Study of Entropy Generation in Fundamental Convective Heat Transfer, *Journal of Heat Transfer, 101* (1979), 4, pp. 718-725
[10] Bejan, A., The Thermodynamic Design of Heat and Mass Transfer Processes and Devices, *Journal of Heat and Fluid Flow, 8* (1987), 4, pp. 258-275
[11] Drost, M. K., White, M. D., Numerical Prediction of Local Entropy Generation in an Impinging Get, *Journal of Heat Transfer, 113* (1991), 4, pp. 823-829
[12] Abu-Nada, E., Numerical Prediction of Entropy Generation in Separated Flows, *Entropy, 7* (2005), 4, pp. 234-252
[13] Abu-Nada, E., Entropy Generation Due to Heat and Fluid Flow in Backward Facing Step Flow with Various Expansion Ratios, *International Journal of Exergy, 3* (2006), 4, pp. 419-435
[14] Abu-Nada, E., Investigation of Entropy Generation over a Backward Facing Step under Bleeding Conditions, *Energy Conversion and Management, 49* (2008), 11, pp. 3237-3242
[15] Bahrami, A., Gandjalikhan Nassab, S. A., Study of Entropy Generation in Laminar Forced Convection Flow over a Forward-Facing Step in a Duct, *International Review of Mechanical Engineering, 4* (2010), 4, pp. 399-404
[16] Kolsi. L., *et al*., The Effect of an External Magnetic Field on The Entropy Generation in Three-Dimensional Natural Convection, *Thermal Science, 14* (2010), 2, pp. 341-352
[17] Gandjalikhan Nassab, S. A., *et al*., Turbulent Forced Convection Flow Adjacent to Inclined Forward Step in a Duct, *International Journal of Thermal Sciences, 48* (2009), 7, pp. 1319-1326
[18] Ansari, A. B., Gandjalikhan Nassab, S. A., Numerical Analysis of Laminar Forced Convection Flow of a Radiating Gas Over an Inclined Forward Facing Step, *International Review of Mechanical Engineering, 5* (2011), 1, pp. 120-127
[19] Ansari, A. B., Gandjalikhan Nassab, S. A., Study of Laminar Forced Convection of Radiating Gas over an Inclined Backward Facing Step under Bleeding Condition Using the Blocked-off Method, *ASME, Journal of Heat Transfer, 133* (2011), 7, 072702
[20] Patankar, S. V., Spalding, D. B., A Calculation Procedure for Heat, Mass and Momentum Transfer in Three-Dimensional Parabolic Flows, *International Journal of Heat and Mass Transfer, 15* (1972), 10, pp. 1787-1806
[21] Patankar, S. V., *Numerical Heat Transfer and Fluid Flow*, Taylor & Francis, Philadelphia, Penn., USA, 1981, Chap. 7
[22] Lari, K., Gandjalikhan Nassabm, S. A. , Modeling of the Conjugate Radiation and Conduction Problem in a 3D Complex Multi-Burner Furnace, *Thermal Science, 16* (2012), 4, pp. 1187-1200
[23] Ansari, A. B., Gandjalikhan Nassab, S. A., Forced Convection of Radiating Gas over an Inclined Backward Facing Step Using the Blocked-off Method, *Thermal Science 17* (2013), 3, pp. 773-786

Paper submitted: May 31, 2011
Paper revised: January 20, 2012
Paper accepted: February 8, 2012